Minjiangite, BaBe$_2$(PO$_4$)$_2$, a new mineral from Nanping No. 31 pegmatite, Fujian Province, southeastern China

C. Rao[1,*], F. Hatert[2], R. C. Wang[3], X. P. Gu[4], F. Dal Bo[2] and C. W. Dong[1]

[1] Department of Earth Sciences, Zhejiang University, 310027 Hangzhou, P.R. China
[2] Laboratoire de Minéralogie, B18, Université de Liège, B–4000 Liège, Belgium
[3] State Key Laboratory for Mineral Deposits Research, School of Earth Sciences and Engineering, Nanjing University, 210093 Nanjing, P.R. China
[4] School of Earth Sciences and Info-physics, Central South University, Changsha, 410083 Hunan, P.R. China

ABSTRACT

Minjiangite, ideally BaBe$_2$(PO$_4$)$_2$, is a new mineral species which has been found in the Nanping No. 31 pegmatite, Fujian Province, southeastern China. It occurs in the fractures of montebrasite from pegmatite zone IV, and is associated with quartz, muscovite, hydroxylapatite and palermoite. Minjiangite forms subhedral to euhedral white crystals from 5 to 200 μm long, transparent to translucent, with a vitreous lustre. The estimated Mohs hardness is ∼6, the tenacity is brittle and no cleavage was observed. The calculated density is 3.49 g/cm^3. Optically, minjiangite is uniaxial (+), with ω = 1.587(3), ε = 1.602(2) (λ = 589 nm). Electron-microprobe analyses (average of 8) give P$_2$O$_5$ 40.16, BaO 43.01, BeO 14.06 (measured by Secondary Ion Mass Spectrometry), SiO$_2$ 0.17, CaO 0.17, SrO 0.08, FeO 0.03, MgO 0.01, TiO$_2$ 0.07, K$_2$O 0.05, Na$_2$O 0.11, total 97.92 wt.%. The empirical formula, calculated on the basis of 8 O a.p.f.u., is (Ba$_{0.99}$Ca$_{0.01}$Na$_{0.01}$)$_{\Sigma 1.01}$Be$_{1.98}$(P$_{1.99}$Si$_{0.01}$)$_{\Sigma 2.00}$O$_8$. The powder X-ray diffraction (XRD) pattern of minjiangite perfectly fits that of synthetic BaBe$_2$(PO$_4$)$_2$; the strongest eight lines of the powder XRD pattern of the natural phosphate [*d* in Å (*I*)(*hkl*)] are: 3.763(100)(101); 2.836(81.3)(102); 2.515(32.3)(110); 2.178(25.6)(200); 2.1620(19)(103); 2.090(63.9)(201); 1.770(16.2)(113); 1.507(25.4)(212). Unit-cell parameters, refined from the powder XRD pattern of natural minjiangite, are *a* = 5.030(8), *c* = 7.467 (2) Å, *V* = 163.96(3) Å^3. These unit-cell parameters confirm that minjiangite is the natural analogue of synthetic BaBe$_2$(PO$_4$)$_2$ (*P*6/*mmm*, *a* = 5.029(1), *c* = 7.466 (1) Å, *V* = 163.52(1) Å^3, *Z* = 1); its crystal structure is topologically similar to that of dmisteinbergite, CaAl$_2$Si$_2$O$_8$, a hexagonal polymorph of anorthite. The formation of minjiangite is related to the hydrothermal alteration of montebrasite by late Ba- and Be-rich fluids.

KEYWORDS: minjiangite, BaBe$_2$(PO$_4$)$_2$, new phosphate mineral species, Nanping No. 31 pegmatite, Fujian province, China.

Introduction

THE new mineral minjiangite, with an ideal composition BaBe$_2$(PO$_4$)$_2$, was discovered in the Nanping No. 31 pegmatite, Fujian province, southeastern China. Phosphate assemblages from this pegmatite were recently re-examined, leading to a description of transformation sequences affecting triphylite (Rao *et al.,* 2014*a*), and to the definition of the new mineral species strontiohurlbutite (Rao *et al.,* 2014*b*). Minjiangite occurs in the Be-rich secondary assemblages observed in the Nanping No. 31 pegmatite.

Due to the very small size of minjiangite crystals, it was impossible to investigate the crystal structure of the mineral directly. However, Dal Bo *et al.* (2014) obtained a synthetic compound with composition BaBe$_2$(PO$_4$)$_2$ hydrothermally, which
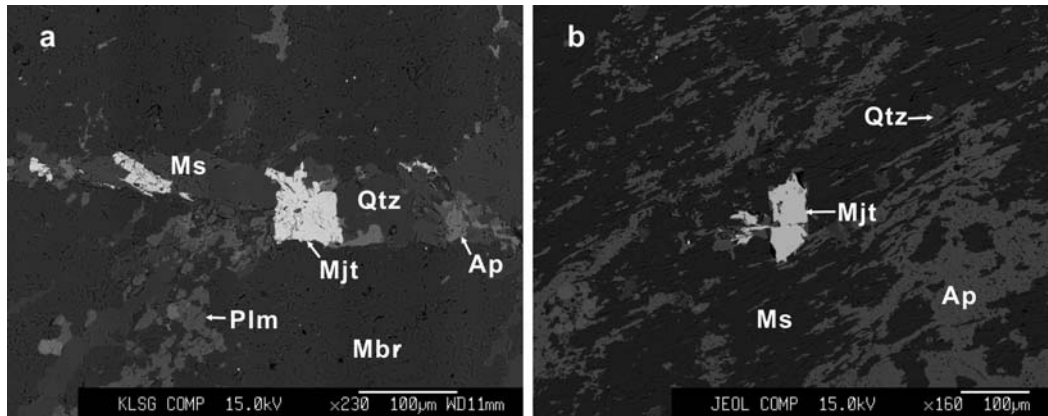
* E-mail: canrao@zju.edu.cn

FIG. 1. Backscattered electron images showing the occurrence and mineral associations of minjiangite. (*a*) Subhedral to euhedral minjiangite is associated with muscovite, quartz, apatite and palermoite in a fracture of montebrasite from Zone IV. (*b*) Euhedral minjiangite associated with muscovite and apatite. Mjt – minjiangite, Mbr – montebrasite, Plm – palermoite, Ms – muscovite, Ap – apatite, Qtz – quartz.

shows a powder XRD pattern identical to that of minjiangite. Consequently the crystal structure of minjiangite is described by comparison to that of this synthetic analogue, for which we also report here a complete set of optical data.

The mineral is named after the Minjiang River, located near the Nanping pegmatite; this river is the largest occurring in Fujian province. The species and the name have been approved by the International Mineralogical Association (IMA) Commission on New Minerals, Nomenclature and Classification (CNMNC) (IMA 2013-021, Rao *et al.*, 2013). The holotype specimen is deposited at the Geological Museum of China, Beijing, China, catalogue number M11842. A cotype of natural minjiangite is deposited at the Laboratory of Mineralogy, University of Liège (catalogue number 20390), as well as the synthetic crystal used by Dal Bo *et al.* (2014) for single-crystal structure determination (catalogue number 20386).

Occurrence and paragenesis

The new mineral was found in the No. 31 pegmatite of Nanping pegmatite field, located in the south-eastern margin of the Caledonian folded belt in the northwest Fujian Province, southeastern China (118°06′ E, 26°40′ N). The geology and petrology of the pegmatite field is as described by Li *et al.* (1983) and Yang *et al.* (1987). The No. 31 pegmatite is a highly evolved spodumene-type pegmatite with strong mineralization of Nb, Ta, Sn,

Be and Li in this pegmatite field; it consists of five mineralogical-textural zones from the outermost zone inwards (Yang *et al.*, 1987; Rao *et al.*, 2009, 2011): Zone I (quartz – albite – muscovite zone), Zone II (saccharoidal albite ± muscovite zone); Zone III (quartz – coarse albite – spodumene zone); Zone IV (quartz – spodumene – amblygonite zone); and Zone V (blocky quartz – K-feldspar zone). The rock samples of minjiangite were collected on the dumps from the mine opening at the 515 m level. On the basis of the mineral assemblages observed, minjiangite occurs in Zone IV (quartz – spodumene – amblygonite zone).

Minjiangite forms subhedral to euhedral crystals, 5 to 200 μm long (usually 20 to 40 μm) and 5 to 50 μm wide. The crystals occur along fractures cutting montebrasite crystals from Zone IV (Fig. 1*a*); they are produced by alteration of montebrasite, during a late hydrothermal stage during which Ba and Sr were remobilized. Backscattered electron (BSE) images show that the crystals are homogeneous; the associated minerals mainly include quartz, muscovite, hydroxylapatite and palermoite. In another sample, minjiangite occurs as isolated grains included in an intimate mixture of muscovite, quartz and hydroxylapatite (Fig. 1*b*).

Physical and optical properties

The crystals of minjiangite are white, transparent to translucent and have vitreous lustre. The estimated Mohs hardness is ~6, the tenacity is brittle and no

cleavage was observed. Owing to the small grain-size, the density and optical properties were not measured directly on natural minjiangite. The density, calculated from the empirical formula and unit-cell parameters refined from powder XRD data, is 3.49 g/cm^3. Synthetic $BaBe_2(PO_4)_2$ is optically uniaxial (+), with $\omega = 1.587(3)$ and $\varepsilon = 1.602(2)$ ($\lambda = 589$ nm). It is non-fluorescent under shortwave (254 nm) and longwave (366 nm) ultra-violet light. The compatibility index, deduced from the calculated density, is $1 - (K_P/K_C) = -0.014$, which corresponds to the 'superior' category (Mandarino, 1981).

Raman and infrared spectroscopies

The Raman spectrum of minjiangite was collected using a Renishaw RM2000 Laser Raman microprobe in the State Key Laboratory for Mineral Deposits Research at Nanjing University. A 514.5 nm Ar$^+$ laser, with a surface power of 5 mW, was used for exciting the radiation; silicon (520 cm^{-1} Raman shift) was used as a standard. Several Raman spectra were acquired from 100 to 1800 cm^{-1}, and the accumulation time for each spectrum was 60 s. Five crystals of minjiangite from polished thin-section chips were observed. The Raman spectrum of minjiangite is characterized by the strong sharp peak at 1050 cm^{-1}, medium sharp peaks at 1233, 491 and 478 cm^{-1}, and weak sharp peaks at 328 and 189 cm^{-1}, respectively (Fig. 2). The major peak at 1050 and the medium sharp peak at 478 cm^{-1} correspond to the stretching and bending modes of (PO$_4$) groups, respectively. The Be–O vibration modes are probably at 1233 and 491 cm^{-1}. Raman shifts at 189 and 328 cm^{-1} are assigned to Ba–O bending vibrations.

An infrared spectrum (400 to 4000 cm^{-1}) was also obtained on a Nicolet 5700 FTIR spectrometer coupled with a Continuum microscope installed at the University of Science and Technology of China, using a KBr beam-splitter and a liquid-nitrogen cooled MCT-A detector. All measurements were carried out using reflection techniques. The representative infrared spectrum of minjiangite is given in Fig. 3, and shows bands at 1375, 1363, 1339 cm^{-1} (BeO$_4$ stretching), 1101, 1068, 1027 cm^{-1} (PO$_4$ stretching), 781 and 730 cm^{-1} (BeO$_4$ bending). These assignments are in good agreement with those established by Dal Bo *et al.* (2014) for synthetic $BaBe_2(PO_4)_2$; the broadening of absorption bands is attributed to the disordered distribution of Be and P on the tetrahedral sites of the minjiangite structure (see below).

Chemical composition

The chemical composition of minjiangite was obtained with a JEOL JXA-8100M electron microprobe (wavelength dispersive spectroscopy mode, 15 kV, 20 nA, beam diameter 1 μm) at the State Key Laboratory for Mineral Deposits Research, Nanjing University. The following
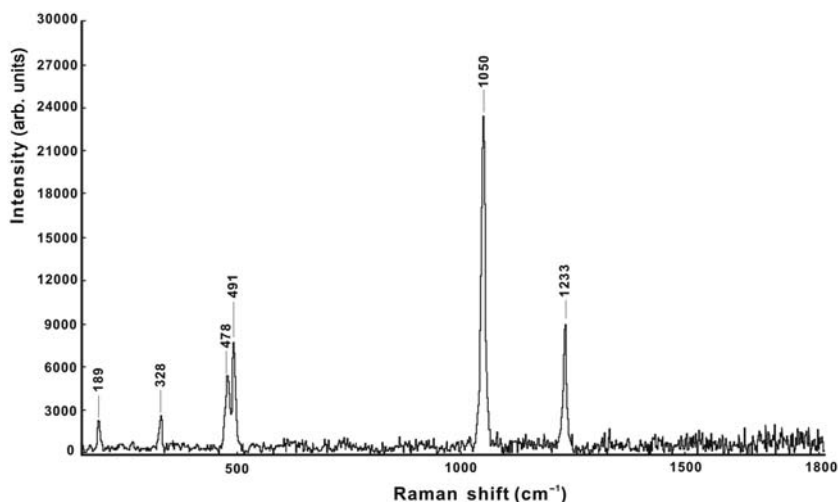
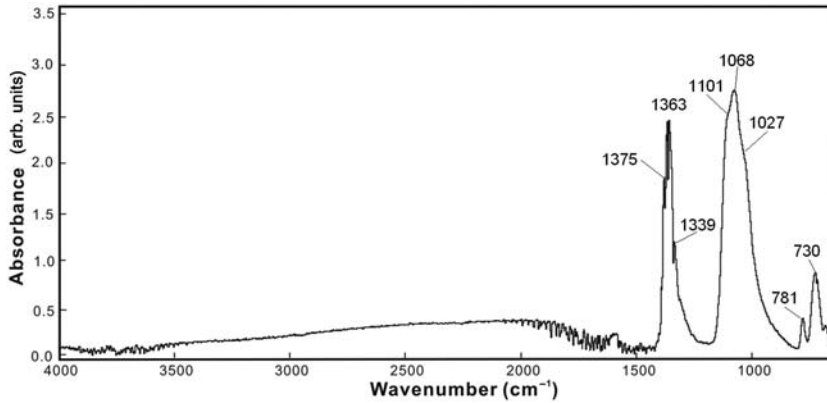

FIG. 2. The Raman spectrum of minjiangite.

1197

FIG. 3. The infrared spectrum of minjiangite.

standards were used: synthetic $Ba_3(PO_4)_2$ ($BaL\alpha$, $PK\alpha$), synthetic $SrSO_4$ ($SrL\alpha$) and hornblende ($SiK\alpha$, $CaK\alpha$, $FeK\alpha$, $MgL\alpha$, $TiK\alpha$, $KK\alpha$, $NaL\alpha$). Matrix corrections were performed with the *PAP* method (Pouchou and Pichoir, 1984); the low analytical total may be due to the presence of large amounts of BeO, which were not taken into account in the matrix absorption corrections.

The BeO content was measured using secondary ion mass spectrometry with a CAMECA NanoSIMS 50L at the Institute of Geology and Geophysics, China Academy of Sciences. A relatively high beam current (500 pA) was used initially to pre-sputter 12 μm × 12 μm of the matrix area. The measurements were undertaken in raster imaging mode by scanning a focused Cs^+ primary

ion beam (30 pA, 0.5 μm diameter) over 10 μm × 10 μm matrix area within the pre-sputtered regions. Negative secondary ions $^9Be^-$, $^{16}OH^-$, $^{18}O^-$, $^{31}P^-$, $^{19}F^-$ were collected simultaneously, along with secondary electrons (SE). Synthetic $BaBe_2(PO_4)_2$ crystals, which have been confirmed by single-crystal XRD in the Laboratory Mineralogy, Liège University (Belgium) were used as the standard sample. The calibration factor for Be in the standard was obtained through the calculation of the experimental Be ion yield, having chosen O as the inner element for the matrix. Thus we derived the ratio (Be/O), defined as $(Be^-/O^-)/((Be(at.)/O(at.))$ where Be^- and O^- are the current intensities detected at the electron multiplier and (at.) is the elemental atomic concentration. The ratio (Be/O)

TABLE 1 Chemical composition of minjiangite.

	Wt.%	Range	SD	Empirical formula (a.p.f.u.)	
P_2O_5	40.16	39.51–40.78	0.52	P	1.993
BaO	43.01	42.42–43.74	0.33	Ba	0.988
BeO*	14.06	–	0.02	Be	1.980
SiO_2	0.17	0–0.41	0.18	Si	0.010
CaO	0.17	0.02–0.37	0.12	Ca	0.010
SrO	0.08	0.01–0.24	0.08	Sr	0.003
FeO	0.03	0–0.07	0.03	Fe^{2+}	0.001
MgO	0.01	0–0.02	0.01	Mg	0.001
TiO_2	0.07	0.0–0.19	0.07	Ti	0.003
K_2O	0.05	0.02–0.11	0.03	K	0.004
Na_2O	0.11	0.06–0.13	0.03	Na	0.012
Total	97.92				

* The BeO content was measured by secondary ion mass spectrometry.
SD – Standard deviation. a.p.f.u. – atoms per formula unit.

was then used to calculate the Be concentration in minjiangite; additionally, lithium was confirmed to be absent from the mineral.

The chemical analysis of minjiangite is given in Table 1. The empirical formula, calculated on the basis of 8 O atoms per formula unit, is $(Ba_{0.99}Ca_{0.01}Na_{0.01})_{\Sigma1.01}Be_{1.98}(P_{1.99}Si_{0.01})_{\Sigma2.00}O_8$. The simplified formula is $BaBe_2(PO_4)_2$, which requires BeO 14.49, BaO 44.40, P_2O_5 41.11, total 100.00 wt.%.

Powder X-ray diffraction

The powder XRD pattern of minjiangite was collected from micro-diffraction data of two crystals, on a RIGAKU D/max Rapid IIR micro-diffractometer ($CuK\alpha$, $\lambda = 1.54056$ Å) at the School of Earth Sciences and Info-physics, Central South University, China. The micro-diffractometer was operated with a Gandolfi-like motion, under 48 kV and 25 mA, using a 0.05 mm diameter collimator; total exposure time was 5 hr. The structural model for synthetic $BaBe_2(PO_4)_2$ crystals (see below) was used to index the powder XRD pattern of minjiangite (Table 2). The stronger eight lines of the powder XRD pattern [d in Å (I)(hkl)] are: 3.763(100)(101); 2.836(81.3)(102); 2.515(32.3)(110); 2.178(25.6)(200); 2.1620(19)(103); 2.090(63.9)(201); 1.770(16.2)(113); 1.507(25.4)(212). The powder XRD data of minjiangite give the following unit-cell parameters, calculated with the least-squares refinement program *LCLSQ 8.4* (Burnham, 1991): $a = 5.030(8)$, $c = 7.467(2)$ Å, $V = 163.96(3)$ Å^3, $Z = 1$, space group $P6/mmm$.

Crystal structure determination

The powder XRD pattern of minjiangite is similar to that of synthetic $BaBe_2(PO_4)_2$; consequently, the structural model of this phosphate can be assumed to be identical to that of minjiangite. Single crystals of $BaBe_2(PO_4)_2$ were synthesized by Dal Bo *et al.* (2014) under hydrothermal conditions; they are colourless, attain 2 mm in diameter and show a morphology of hexagonal tablets. Single-crystal XRD data were collected by these authors on this synthetic phase; unit-cell parameters are $a = 5.029(1)$, $c = 7.466(1)$ Å, $V = 163.51(1)$ Å^3 ($Z = 1$, space group $P6/mmm$). The structure was solved to $R_1 = 0.021$; further experimental details, as well as a table with atomic coordinates and anisotropic displacement parameters, are available in Dal Bo *et al.* (2014).

The crystal structure is based on a double layer of tetrahedra containing both Be and P. These tetrahedra are assembled in six-membered rings, which are stacked parallel to the c axis, forming channels (Fig. 4). In the $a–b$ plane, each ring is connected to six adjacent rings to form an infinite layer. Along the **c** direction, tetrahedra are connected by sharing their apical oxygen to form a double layer; the Ba atoms are located in a 12-coordinated polyhedron occurring between two double layers. This type of Ba polyhedron shows a very regular hexagonal shape, with 12 identical Be–O(2) bonds of 2.975(2) Å long (Fig. 5). Refinement of the site occupancy factors on the tetrahedral sites indicates that these sites are occupied simultaneously by Be and P (constrained occupancy factors: 0.5 P + 0.5 Be). The average bond length for these tetrahedral sites is 1.563 Å (Dal Bo *et al.*, 2014), which is longer than the standard bond length expected for a PO_4 tetrahedra (1.55 Å). This disordered Be–P distribution is confirmed by the broad absorption bands observed in the infrared spectrum of minjiangite (Fig. 3).

Discussion

Minjiangite is the natural analogue of synthetic $BaBe_2(PO_4)_2$, and belongs to the group of phosphate minerals without additional anions, without water and with small cations (Strunz 8. AA.35; Dana 38.3.6.3.). It shows a general formula $M^{2+}Be_2P_2O_8$, stoichiometrically identical to that of hurlbutite-group minerals, $(Ca,Sr)Be_2P_2O_8$ (Mrose, 1952; Rao *et al.*, 2014*b*). However, minjiangite crystallizes in the hexagonal system, and shows a crystal structure significantly different from those of monoclinic hurlbutite-group minerals (Mrose, 1952; Rao *et al.*, 2014*b*; Dal Bo *et al.*, 2014). The crystal structure of minjiangite is topologically similar to that of the hexagonal feldspar dmisteinbergite ($CaAl_2Si_2O_8$: Takéuchi and Donnay, 1959; Chesnokov *et al.*, 1990).

A peculiar feature of the crystal structure of synthetic $BaBe_2(PO_4)_2$ is the presence of a completely disordered distribution of P and Be atoms on the tetrahedral sites, leading to occupancy factors of 0.5 P and 0.5 Be on that site (Dal Bo *et al.*, 2014). Such P/Be disorder has never been reported to date (Hawthorne and Huminicki, 2002; Rao *et al.*, 2014*b*; Dal Bo *et al.*, 2014), and seems unlikely, due to the charge difference of 3+ between P and Be, and to the significant difference in effective ionic radii (e.i.r.) between these two

TABLE 2 Powder XRD pattern of minjiangite.

Minjiangite							Synthetic BaBe$_2$(PO$_4$)$_2$*	
d_{meas} (Å)	I (%)	d_{cal} (Å)	I_{calc} (%)	h	k	l	d$_{meas}$ (Å)	I (%)
4.352	3.8	4.357	4.0	1	0	0	4.364	4.4
3.763	100.0	3.766	100.0	1	0	1	3.768	100.0
2.836	81.3	2.841	62.0	1	0	2	2.839	61.4
2.515	32.3	2.516	28.6	1	1	0	2.519	25.6
2.384	7.8	2.385	5.9	1	1	1	2.388	7.5
2.178	25.6	2.179	13.8	2	0	0	2.183	15.3
2.162	19.0	2.167	19.7	1	0	3	2.164	25.7
2.090	63.9	2.092	27.8	2	0	1	2.094	40.8
1.883	11.8	1.883	3.4	2	0	2	1.884	4.3
1.867	3.2	1.873	6.5	0	0	4	1.869	9.7
1.770	16.2	1.772	16.0	1	1	3	1.772	24.5
1.608	23.7	1.608	17.8	2	1	1	1.611	18.26
1.507	25.4	1.508	18.3	2	1	2	–	–
1.453	11.2	1.452	6.2	3	0	0	–	–
1.414	5.0	1.417	5.5	1	0	5	–	–
1.374	10.8	1.375	7.9	2	1	3	–	–
1.258	12.5	1.258	6.4	2	2	0	–	–
1.256	13.1	1.256	4.7	3	0	3	–	–
1.233	9.3	1.235	3.0	2	0	5	–	–
1.150	7.9	1.150	7.4	3	1	2	–	–
1.148	9.0	1.148	3.7	3	0	4	–	–
0.966	5.7	0.966	3.0	3	2	2	–	–

* Powder XRD pattern of the compound synthesized by Dal Bo *et al.* (2014), measured on a Panalytical PW-3710 diffractometer equipped with an Fe$K\alpha$ X-ray tube ($\lambda = 1.9373$ Å).

cations (0.27 Å for Be and 0.17 Å for P; Shannon, 1976). However, similar disordered distributions were previously observed between Be and trivalent cations (Al^{3+}, e.i.r. = 0.39 Å; B^{3+}, e.i.r. = 0.11 Å), and between Be and monovalent cations (Li$^+$, e.i.r. = 0.590 Å) (Hawthorne and Huminicki, 2002). Moreover, Si/Be, Al/Be, or Si/Al/Be disordered distributions were reported in some tetrahedral sites of semenovite (Mazzi *et al.*, 1979), khmaralite (Barbier *et al.*, 1999), makarochkinite (Grew *et al.*, 2005), oftedalite (Cooper *et al.*, 2006) and welshite (Grew *et al.*, 2007).

Four arguments confirm the Be/P disordered distribution observed in minjiangite. (1) Even if the charge difference between Be and P is extremely large, the difference in ionic radii, e.i.r. Be^{2+} – e.i.r. P^{5+} = 0.10 Å, is relatively small, compared to other trivalent and monovalent cations substituting to Be: e.i.r. Be^{2+} – e.i.r. Al^{3+} = –0.12 Å, e.i.r. Be^{2+} – e.i.r. B^{3+} = 0.16 Å, e.i.r. Be^{2+} – e.i.r. Li$^+$ = –0.32 Å. (2) According to Fig. 4, each oxygen, located in the basal level of the tetrahedral layers, is bonded to two tetrahedral cations, as well as to two Ba atoms. Theoretical bond-valence calculations indicate that each 12-coordinated Ba^{2+} atom shares $2/12 = 0.1667$ valence units (vu) with the oxygen atoms; as a consequence, each basal oxygen atoms shares $2 \times 0.1667 = 0.3333$ vu with Ba atoms. The remaining bond valence, $2 - 0.3333 = 1.6667$, is consequently shared between the two tetrahedral cations. Each tetrahedral cation is coordinated by three basal oxygen atoms, and by one apical oxygen atom which is only shared between two tetrahedral sites; the ideal bond-valence sum for the tetrahedral cations is therefore $[3 \times (1.6667/2)] + 1 = 3.5$, corresponding exactly to the value obtained for the observed occupancy $0.5\text{Be}^{2+} + 0.5\text{P}^{5+}$. (3) Refined site-scattering values, as well as (Be,P)–O bond distances, are in good agreement with a disordered Be/P distribution. (4) The infrared spectrum of synthetic BaBe$_2$(PO$_4$)$_2$ shows very broad absorption bands, compared to the spectra of synthetic
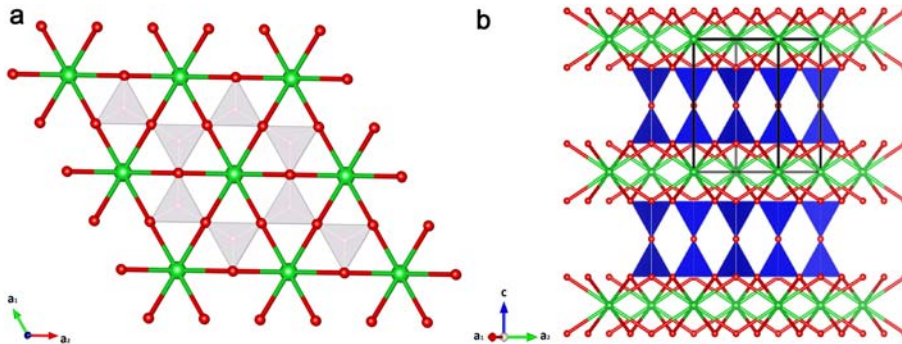
1200

FIG. 4. The crystal structure of synthetic minjiangite, based on double $(Be_2P_2)O_8$ layers and a BaO_{12} layer (after Dal Bo *et al*., 2014. Drawn using the *VESTA 3* program; Momma and Izumi, 2011).

$CaBe_2(PO_4)_2$, $SrBe_2(PO_4)_2$ and $PbBe_2(PO_4)_2$ compounds (Dal Bo *et al*., 2014).

As observed in Fig. 1, minjiangite formed during hydrothermal processes affecting the Nanping No. 31 pegmatite; it constitutes one of the hydrothermal alteration products of primary montebrasite in Zone IV. Indeed, hydrothermal fluids were widespread in the Nanping No. 31 pegmatite, leading to the breakdown of most of the primary minerals, such as spodumene, amblygonite, triphylite, K-feldspar and beryl (Yang *et al*. 1994; Rao *et al*. 2011, 2014*a*). The presence of Be and Ba in the hydrothermal fluids responsible for the formation of minjiangite is due to the alteration of beryl and Ba-rich K-feldspar. Other secondary Ba-bearing minerals, such as kulanite, $BaFe_2^{2+}Al_2(PO_4)_3(OH)_3$ and fluorarrojadite-(BaNa), $Na_2CaBaFe^{2+}Fe_{13}^{2+}Al$

$(PO_4)_{11}(PO_3OH)F_2$, were also observed as alteration products of primary montebrasite from Zone IV, confirming the presence of Ba-rich fluids. Yang *et al*. (1994) suggested that primary montebrasite in the Nanping pegmatite formed from 200 to 295°C, on the basis of fluid inclusion studies. Consequently, minjiangite, which formed after montebrasite, probably crystallized at <275°C, a temperature in good agreement with the synthesis temperature of $BaBe_2(PO_4)_2$, corresponding to 200°C.

Acknowledgements

References

Barbier, J., Grew, E.S., Moore, P.B. and Su, S. (1999) Khmaralite, a new beryllium-bearing mineral related to sapphirine: a superstructure resulting from partial ordering of Be, Al, and Si on tetrahedral sites. *American Mineralogist*, **84**, 1650–1660.

Burnham, C.W. (1991) *LCLSQ version 8.4, least-squares refinement of crystallographic lattice parameters.* Department of Earth and Planetary Sciences, Harvard University, Cambridge, Massachusetts, USA.

Chesnokov, B.V., Lotova, E.V., Nigmatulina, E.N., Pavlyuchenko, V.S. and Bushmakin, A.F. (1990) Dmisteinbergite $CaAl_2Si_2O_8$ (hexagonal) – a new mineral. *Zapiski Vsesoyuznogo Mineralogicheskogo Obshchestva*, **119**, 43–46 [in Russian].
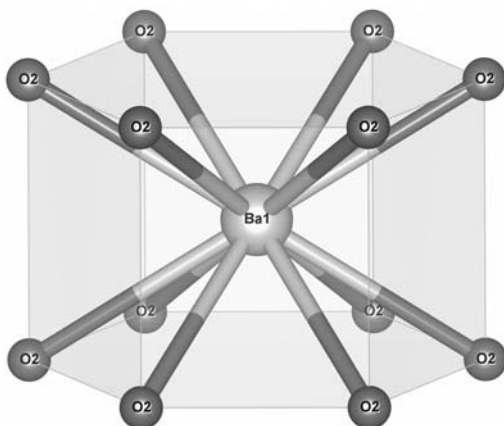

FIG. 5. Ba^{2+} in a 12-coordinated polyhedron (after Dal Bo *et al*., 2014. Drawn using the *VESTA 3* program; Momma and Izumi, 2011).

Cooper, M.A., Hawthorne, F.C., Ball, N.A. and Cerný, P. (2006) Oftedalite, $(Sc,Ca,Mn^{2+})_2K(Be,Al)_3Si_{12}O_{30}$, a new member of the milarite group from the Heftetjern pegmatite, Tordal, Norway: description and crystal structure. *The Canadian Mineralogist*, **44**, 943–949.

Dal Bo, F., Hatert, F. and Baijot, M. (2014) Crystal Chemistry of synthetic $M^{2+}Be_2P_2O_8$ (M^{2+} = Ca, Sr, Pb, Ba) beryllophosphates. *The Canadian Mineralogist*, **52**, 337–350.

Grew, E.S., Barbier, J., Britten, J., Yates, M.G., Polyakov, V.O., Shcherbakova, E.P., Hålenius, U. and Shearer, C.K. (2005) Makarochkinite, $Ca_2Fe_4^{2+}Fe^{3+}TiSi_4BeAlO_{20}$, a new beryllosilicate member of the aenigmatite-sapphirine-surinamite group from the Il'men mountains (southern Urals), Russia. *American Mineralogist*, **90**, 1402–1412.

Grew, E.S., Barbier, J., Britten, J., Hålenius, U. and Shearer, C.K. (2007) The crystal chemistry of welshite, a non-centrosymmetric (P1) aenigmatite-sapphirine-surinamite group mineral. *American Mineralogist*, **92**, 80–90.

Hawthorne, F.C. and Huminicki, D.M.C. (2002) The crystal chemistry of beryllium. Pp. 333–404 in: *Beryllium: Mineralogy, Petrology, and Geochemistry* (E.S. Grew, editor). Reviews in Mineralogy & Geochemistry, **50**. Mineralogical Society of America and the Geochemical Society, Washington DC.

Li, Z.L., Zhang, J.Z., Wu, Q.H. and Ouyang, Z.H. (1983) Geological and geochemical characteristics of a certain pegmatite ore field of rare metals in Fujian Province. *Mineral Deposits*, **2**, 49–58 [in Chinese with English abstract].

Mandarino, J.A. (1981) The Gladstone-Dale relationship. IV. The compatibility concept and its application. *The Canadian Mineralogist*, **19**, 441–450.

Mazzi, F., Ungaretti, L., Dal Negro, A., Peterson, O.V. and Rönsbo, J.G. (1979) The crystal structure of semenovite. *American Mineralogist*, **64**, 202–210.

Momma, K. and Izumi, F. (2011) VESTA 3 for three-dimensional visualization of crystal, volumetric and morphology data. *Journal of Applied Crystallography*, **44**, 1272–1276.

Mrose, M.E. (1952) Hurlbutite, $CaBe_2(PO_4)_2$, a new mineral. *American Mineralogist*, **37**, 931–940.

Pouchou, J.L. and Pichoir, F. (1984) Extension des possibilités quantitatives de la microanalyse par une formulation nouvelle des effets de matrice. *Journal de Physique*, **45**, 17–20.

Rao, C., Wang R.C., Hu, H. and Zhang, W.L. (2009) Complex internal texture in oxide minerals from the Nanping No. 31 dyke of granitic pegmatite, Fujian Province, southeastern China. *The Canadian mineralogist*, **47**, 1195–1212.

Rao, C., Wang, R.C. and Hu, H. (2011) Paragenetic assemblages of beryllium silicates and phosphates from the Nanping no. 31 granitic pegmatite dyke, Fujian province, southeastern China. *The Canadian Mineralogist*, **49**, 1175–1187.

Rao, C., Hatert, F., Wang, R.C., Gu, X.P., Dal, B.F. and Dong, C.W. (2013) Minjiangite, IMA 2013-021. CNMNC Newsletter No. 16, August 2013, page 2705; *Mineralogical Magazine*, **77**, 2695–2709.

Rao, C., Wang, R.C., Hatert, F. and Baijot, M. (2014*a*) Hydrothermal transformations of triphylite from the Nanping No. 31 pegmatite dyke, southeastern China. *European Journal of Mineralogy*, **26**, 179–188.

Rao, C., Wang, R.C., Hatert, F., Gu, X., Ottolini, L., Hu, H., Dong, C., Dal Bo, F. and Baijot, M. (2014*b*) Strontiohurlbutite, $SrBe_2(PO_4)_2$, a new mineral from Nanping no. 31 pegmatite, Fujian Province, Southeastern China. *American Mineralogist*, **99**, 494–499.

Shannon, R.D. (1976) Revised effective ionic radii and systematic studies of interatomic distances in halides and chalcogenides. *Acta Crystallographica*, **A32**, 751–767.

Takéuchi, B.Y. and Donnay, G. (1959) The crystal structure of hexagonal $CaAl_2Si_2O_8$, *Acta Crystallographica*, **12**, 465–470.

Yang, Y.Q., Ni, Y.X., Guo, Y.Q., Qiu, N.M., Chen, C.H., Cai, C.F., Zhang, Y.P., Liu, J.B. and Chen, Y.X. (1987) Rock-forming and ore-forming characteristics of the Xikeng granitic pegmatites in Fujian Province. *Mineral Deposits*, **6**, 10–21 [in Chinese with English abstract].

Yang, Y.Q., Wang, W.Y., Ni, Y.X., Chen, C.H. and Zhu, J.H. (1994) Phosphate minerals and their geochemical evolution of granitic pegmatite in Nanping, Fujian Province. *Geology of Fujian*, **13**, 215–226 [in Chinese with English abstract].